ISSN 1063-7850, Technical Physics Letters, 2019, Vol. 45, No. 3, pp. 267–270. © Pleiades Publishing, Ltd., 2019.
Russian Text © G.V. Kuznetsov, P.A. Strizhak, 2019, published in Pis'ma v Zhurnal Tekhnicheskoi Fiziki, 2019, Vol. 45, No. 6, pp. 23–26.

Collisions between Liquid Drops of Various Shapes in a Gas Flow

G. V. Kuznetsov[a] and P. A. Strizhak[a]*

[a] *Tomsk Polytechnic University, Tomsk, 634050 Russia*

**e-mail: pavelspa@tpu.ru*

Received August 9, 2018; revised December 21, 2018; accepted December 21, 2018

Abstract—We have experimentally studied the interaction between water drops of various surface configurations moving in a gas medium. Results of high-speed video monitoring provide a database on these collisions (in coagulation, expansion, and fragmentation regimes) for particles of spherical, oblate, and elongated ellipsoids. It is established that a determining role belongs to the surface configuration of drops (in addition to traditional notions about the influence of their dimensions, velocities, and angle of attack). The values of Weber numbers have been calculated for description of the conditions of interaction between drops of various shapes.

DOI: 10.1134/S1063785019030301

Modern notions about the collisions of liquid drops in a gas medium (as summarized in monographs [1–3]) have been formulated based on the analysis of results of experiments performed using two main approaches. The first (phenomenological) approach consists in monitoring of the interaction between two drops of different dimensions moving with various velocities (sometimes one drop is immobilized by suspending it on a holder, while the other moves at a preset velocity on a given trajectory) [4, 5]. In the second (statistical) approach, an aerosol cloud is generated and monitored, after which frame samples are used to create a database on the number of collisions and variants of their outcome, and the corresponding frequencies are calculated [6, 7]. The main attention in conducting these experiments is devoted to monitoring the dimensions, velocities, trajectories, and angles of interaction between drops. Using dimensionless processing of experimental results [4], it is possible to determine typical intervals of variation of the Weber numbers of colliding drops, which correspond to their coagulation, expansion, and fragmentation. However, according to the results of experiments [8], it can also be concluded that liquid drops during flight exhibit continuous deformation and take various forms (six to eight variants) significantly different from spherical, including drop-shaped, ellipsoidal, etc. Therefore, it would be of interest to study the collisions between drops having different surface configurations.

This Letter presents the results of our experiments aimed at determining differences between the characteristics of collisions between water drops of various shapes moving in air. In contrast to experiments [6–8], we used a scheme with generation of mutually oriented, either copropagating or mutually perpendicular polydisperse aerosol flows. In addition, we have also studied the conditions of collisions between drops in mixing counterflows of aerosol and air. Different directions of aerosol and air flows provide a greater number of possible variants of collision with broad variation of dimensions, velocities, and angles of attack of colliding drops. In this work, the intervals of variation of the parameters of colliding drops were as follows: dimensions (effective radii), 0.1–1 mm velocities, 0.1–10 m/s; angles of collision, $0–\pi/2$.

The process of collision was monitored by a high-speed video camera with a picture format of 1152 × 864 pixels and a frame rate of up to 10000 fps. The camera position relative to the region of flow mixing in a series of experiment was varied so as to obtain 3D patterns. Figure 1 shows typical frames with images of mutually approaching and colliding drops with various surface configurations, including sphere and elongated or oblate ellipsoids. There is a large variety of possible drop shapes and positions during flight. For example, six to eight typical configurations were presented in [8, 9], but experiments in these works showed that drops occurred in configurations of sphere and elongated or oblate ellipsoids for about 70–80% of the flight time.

Similarly to the experiments described in [6, 7], we have selected samples of frames displaying the process of mutual approach of colliding drops in the gaseous medium. All collisions were subdivided into three groups, each group representing one of three possible dominant variants of collision consequences (out-

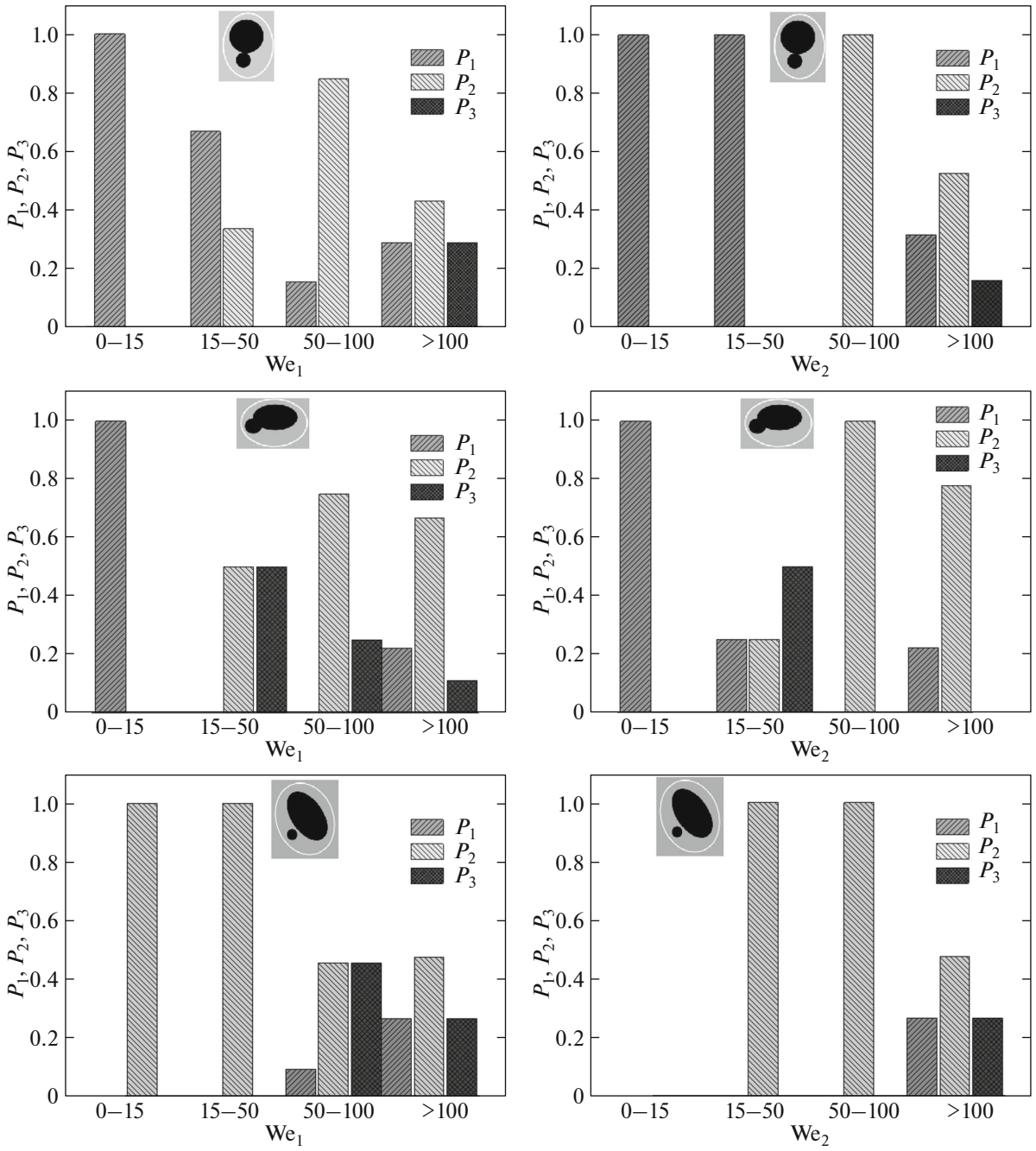

Fig. 1. Frequencies of collision outcomes for drops of various shapes plotted versus Weber numbers for (We_1) projectile, (We_2) target, (P_1) coagulation, (P_2) expansion, and (P_3) fragmentation in three adopted schemes of interaction: sphere–sphere (top row), sphere–elongated ellipsoid (middle row), and sphere–oblate ellipsoid (bottom row).

comes): (i) coagulation (merging), (ii) expansion (collision resulting in the formation of two drops with dimensions corresponding to initial), and (iii) fragmentation (comminution). Then, the frequencies (probabilities) of each particular type of consequences were calculated for each particular variant of event at identical parameters of collisions relative to the total number of events: P_1 (coagulation), P_2 (expansion), and P_3 (fragmentation), the sum of P_1, P_2, and P_3 was equal to unity. The analysis of an experiment was performed by processing no less than 100 interactions between drops under identical conditions.

Processing of the results of experiments yielded the dependences of P_1, P_2, and P_3 values on drop sizes R_d, velocities of motion U_d, and collision angles α_d (analogous to those reported in [6, 7]). These dependences were used to calculate the Weber numbers of

drops approaching each other prior to collision with allowance for the relative velocity of their motion $U_d = (|U_{d1}|^2 + |U_{d2}|^2 - 2|U_{d1}||U_{d2}|\cos(a_d))^{0.5}$: $We_1 = 2\rho R_{d1}|U_d|^2/\sigma$, $We_2 = 2\rho R_{d2}|U_d|^2/\sigma$. The values of parameters U_{d1}, U_{d2}, R_{d1}, and R_{d2} were determined from the corresponding video records. The experimental techniques and error of measurements corresponded to those described in [6, 7]. The images of observed drops were classified with respect to their shapes through comparison to adopted standard configurations. Deviations from average dimensions were only allowed within 5%. The properties of water were set in correspondence with previous experiments at 20°C [4–7]: density $\rho = 10^3$ kg/m^3 and surface tension $\sigma = 72.88 \times 10^{-3}$ kg/s^2.

Figure 1 presents the values of P_1, P_2, and P_3 determined from experimental data obtained in a broad range of collision angles $\alpha_d = 0$–$\pi/2$ (analogous to those used in [4–6]). These P_1, P_2, and P_3 values correspond to the variation of We_1 and We_2 for colliding drops of various shapes (in all cases, the projectile drop shape was close to spherical, while the target drop had configurations of sphere and elongated or oblate ellipsoid). In case of collisions of the sphere–sphere type, dominating P_1 values corresponded to high frequency of the coagulation outcome (see Fig. 1). In the interaction scheme of sphere–oblate ellipsoid, dominating outcome was expansion (P_2) and quite large values were also observed for fragmentation (P_3). Video records showed stable dependence of P_2 and P_3 values on the conditions of collision in the scheme of sphere–oblate ellipsoid. In particular, the effect of a spherical drop in the central part of oblate ellipsoid led to the expansion of drops with retained initial dimensions. The effect of a spherical drop on the side part of oblate ellipsoid led to almost complete disintegration (with the formation of a polydisperse aerosol). Collisions of drops in the scheme of sphere–oblate ellipsoid exhibited dominating P_2 and, especially, P_3 values corresponding to the conditions of intense fragmentation of colliding drops. A decrease in the velocity or size of the projectile drop led to increasing P_2, while P_1 values were small in the entire range of We_1 and We_2.

The values of P_1, P_2, and P_3 exhibit several-fold differences in the sphere–sphere, sphere–elongated ellipsoid, and sphere–oblate ellipsoid for identical We_1 and We_2 values (see Fig. 1). Even more pronounced distinctions were observed for drop interactions in the ellipsoid–ellipsoid scheme. The conditions of interaction between oblate ellipsoids were most significantly different from all other cases (Fig. 1). This was related to instability of the surfaces of drops in this configuration [8] and variety of the possible collision outcomes. In particular, experiments showed that oblate ellipsoids were strongly decelerated in airflow (whereby their velocities decreased several times) as compared to spheres and elongated ellipsoids. This behavior was caused by high values of aerodynamic drag coefficients c_d (on average, 1.2–1.6 times greater than those for spheres and 1.5–2.1 times greater than for elongated ellipsoids [8—10]). As a result, the aerodynamic forces acting upon oblate ellipsoids were substantially stronger [10]. Another significant factor was related to differences between positions of the centers of mass in drops of various configurations. Only maximum sizes and small velocities of oblate ellipsoids demonstrated occasional cases of coagulation outcome (see Fig. 1). Therefore, for intensification of the fragmentation of drops, it is important to manage transformation of their surface by means of rotation, pulsed supply, vibrations, and other effects as described in [8–10].

From comparative analysis of the results presented in Fig. 1 and known data on the limiting values of Weber numbers for various outcomes of interactions—in particular, for collisions of two drops [4, 5] or particles in aerosol [6, 7]—it can be concluded that satisfactory correspondence was only established for interactions in the sphere–sphere scheme. In this scheme, the differences between the transition values of We_1 and We_2 (between different interaction regimes) did not exceed 10–20%. For example, results of experiments [4–7] indicated that the interaction of drops at $0 < We < 0.5$ resulted in the merging of drops under the action of surface tension forces, condition $0.5 < We < 1.5$ led to a rebound (due to a gas interlayer between drops), interval $15 < We < 50$ corresponded to the expansion of drops, $50 < We < 100$ combined expansion and fragmentation depending on the arrangement of the centers-of-mass in colliding drops, and $We > 100$ resulted in stable fragmentation. Our experiments established that ellipsoids have significantly smaller limiting values of We_1 and We_2 corresponding to expansion and fragmentation (see Fig. 1). Only the Weber numbers for coagulation were close in various schemes of collisions at small velocities and sizes of drops.

The significance of the experiments described above consists in establishing differences of We_1 and We_2 values corresponding to most typical surface configurations of drops. The limiting values of Weber numbers corresponding to the transition from coagulation to expansion of spherical drops amounted to 15–25. In the scheme of a sphere–elongated ellipsoid, these values decrease to 10–18, while in the case of a sphere–oblate ellipsoid they fall within 7–11. Taking into account that values of the aerodynamic drag coefficients c_d for drops of various shapes can change from 0.24 to 0.56 [8–10], there is a clear relationship between c_d and the values of P_1, P_2, and P_3. It will be worthwhile to describe this relationship mathematically with allowance for various possible configurations of colliding drops in future investigations. It will also be of benefit to perform experiments with liquids and gases significantly different from water and air

with respect to properties such as viscosity, density, and surface tension. This will probably yield a correction coefficient for transition Weber numbers between the coagulation, expansion, and fragmentation outcomes with allowance for the aerodynamic drag.

This investigation summarizes the results of experiments with drops colliding in air without heating, in contrast to the case studied in [6, 7], where dropwise aerosol was injected into a counterpropagating flow of high-temperature (up to 1000°C) combustion products and the main outcome was the coagulation of colliding drops. Taking into account the results obtained in the present work, it is possible to formulate additional comments explaining the high values of P_1 frequency observed in [6, 7]. First, the counterflow of combustion products significantly retarded drops of aerosol. Second, high temperature intensified the evaporation and favored decrease in the size of drops and their approaching spherical shapes. Third, turbulent pulsations of combustion products chaotically displaced and rotated drops. As a result, the probability of collisions between counterpropagating drops at high relative velocity was small. For these reasons, in experiments with aerosol [6, 7] the values of P_2 and, even more so, of P_3 were significantly lower than P_1. Nevertheless, the role of drop shapes was important even at small We_1 and We_2 values (see Fig. 1). In experiments with two drops [4, 5] and with aerosol [6, 7], proper allowance for the shape factor will lead to significant changes in the P_1, P_2, and P_3 values as functions of We_1 and We_2.

In concluding, the results of experiments showed incomplete correspondence of the existing theory of interaction between liquid drops moving in a gas medium [1–3, 6–10] to real collision processes. This discrepancy is related to the fact that theoretical notions [1–3, 6–10] take into account three main factors (sizes, velocities, and angle of interaction) but ignore the possible influence of drop shapes. At close values of the Weber numbers, various outcomes of collisions between drops are possible depending on their surface configurations (see Fig. 1). It is important to take this circumstance into account in gas–vapor–drop media applications [10] for correctly tuning spray systems.

Acknowledgments. This work was supported in part by the Russian Science Foundation, project no. 18-71-10002.

REFERENCES

1. N. A. Fuks, *The Mechanics of Aerosols* (Akad. Nauk SSSR, Moscow, 1955) [in Russian].
2. D. G. Pazhi and V. S. Galustov, *Fundamentals of Fluid Spraying Technology* (Khimiya, Moscow, 1984) [in Russian].
3. R. I. Nigmatulin, *Dynamics of Multiphase Media* (Vysshaya Shkola, Moscow, 1985) [in Russian].
4. V. A. Arkhipov, G. S. Ratanov, and V. F. Trofimov, Prikl. Mekh. Tekh. Fiz., No. 2, 73 (1978).
5. V. A. Arkhipov, I. M. Vasenin, and V. F. Trofimov, Prikl. Mekh. Tekh. Fiz., No. 3, 95 (1983).
6. R. S. Volkov, G. V. Kuznetsov, and P. A. Strizhak, Tech. Phys. Lett. **41**, 840 (2015).
7. D. V. Antonov, R. S. Volkov, G. V. Kuznetsov, and P. A. Strizhak, Inzh.-Fiz. Zh. **89** (1), 94 (2016).
8. R. S. Volkov, G. V. Kuznetsov, and P. A. Strizhak, Int. J. Heat Mass Transfer **85**, 1 (2015).
9. A. A. Shreiber, A. M. Podvysotsky, and V. V. Dubrovsky, Atom. Sprays **6**, 667 (1996).
10. O. V. Vysokomornaya, G. V. Kuznetsov, and P. A. Strizhak, *Evaporation and Transformation of Droplets and Large Arrays of Liquid when Moving through High-Temperature Gases* (Sib. Otdel. RAN, Novosibirsk, 2016) [in Russian].

Translated by P. Pozdeev